JOURNAL OF VIROLOGY, Oct. 2008, p. 9657–9667 Vol. 82, No. 19
0022-538X/08/$08.00+0 doi:10.1128/JVI.00107-08

Functional Characterization of the Human Immunodeficiency Virus Type 1 Nef Acidic Domain[▽]

Laura L. Baugh, J. Victor Garcia,* and John L. Foster

Department of Internal Medicine, Division of Infectious Diseases, University of Texas Southwestern Medical Center, Dallas, Texas 75390

Received 15 January 2008/Accepted 17 June 2008

The human immunodeficiency virus type 1 (HIV-1) accessory protein Nef downregulates major histocompatibility complex class I (MHC-I) from the cell surface. It has been proposed that the direct interaction of the acidic cluster (AC) of Nef, ^{62}EEEE^{65}, with the furin binding region (fbr) of PACS-1 is crucial for this Nef function. Contrary to this proposal, evidence is presented here that the four glutamates in Nef do not functionally engage the PACS-1 fbr. (i) The binding of Nef to the PACS-1 fbr in vitro is much weaker than the binding of the canonical furin AC to the PACS-1 fbr. (ii) The mutation of two of the four glutamates in Nef's AC to alanines does not alter Nef's ability to downregulate MHC-I, and triply mutated Nefs exhibit 50% activity. (iii) The introduction of lysine into the AC has little effect on Nef function. (iv) The mutation of all four glutamates to alanine does debilitate Nef MHC-I downregulation, but this quadruple mutation also impairs the ability of Nef to regulate p21-activated protein kinase and enhance viral particle infectivity. (v) The replacement of the Nef AC with the bona fide AC from furin results in the loss of the expected regulatory properties of the furin AC. (vi) The insertion of the conformation-disrupting amino acid proline into the Nef AC does not disrupt MHC-I downregulation. Our results are consistent with an alternative model in which ^{62}EEEE^{65} plays a stabilizing role in the formation of a ternary complex between Nef, the MHC-I cytoplasmic domain, and AP-1.

Nef is the most intensely studied of the auxiliary genes of human immunodeficiency virus type 1 (HIV-1) (3, 4, 8, 19, 29). The major reasons for this are Nef's multifunctionality and the highly significant role of Nef in determining pathogenicity (9, 16), which attract researchers with diverse perspectives. Particularly noteworthy in this regard is the ability of Nef to downregulate the major histocompatibility complex class I (MHC-I) from the cell surface. First described by Schwartz et al. in 1996 (31), this phenomenon has yet to be understood mechanistically. Until recently, the prevailing view was that Nef achieves MHC-I downregulation by enhancing the rate of MHC-I endocytosis. Specifically, Thomas and coworkers (5, 6, 13) envision an initial complex between Nef and PACS-2 (termed the NPA model) that forms when the four contiguous glutamate residues (the acidic cluster [AC]) in Nef (^{62}EEEE^{65}) engage the furin binding region (fbr) of PACS-2. PACS-2 may bind to other sorting molecules to target Nef to the *trans*-Golgi network (TGN). The mutation of the four glutamates in Nef to four alanines abrogates the MHC-I downregulation function (10). At the TGN, a second structural motif of Nef, which is proposed to be an SH3 binding domain (^{72}PXXP^{75}), engages an unidentified *src* family kinase (SFK) that displaces PACS-2. The SFK then would bind and phosphorylate ZAP70/Syk on tyrosine, enabling ZAP70/Syk to bind the SH2 domain of phosphatidylinositol 3-kinase (PI3K). The resulting activation of PI3K would lead to elevated levels of phosphatidylinositol (3,4,5)-trisphosphate, the stimulation of the guanine nucleotide exchange factor ARNO, and the GTP loading of ARF6. This completes the train of events initiated by Nef/PACS-2 binding. To achieve MHC-I downregulation, the NPA model continues with activated ARF6 inducing the rapid internalization of MHC-I. For the increased rate of MHC-I internalization to be effective in reducing MHC-I cell surface levels, Nef also blocks the recycling of MHC-I back to the plasma membrane. This last Nef activity is specifically disabled by the M20A mutation (2, 6). In the latest version of the NPA model, an interaction between ^{62}EEEE^{65} and PACS-1 is suggested to play a necessary role by acting downstream of the PACS-2-dependent formation of the SFK-ZAP70/Syk-PI3K complex (5). In summary, the NPA account of the ultimate sequestration of MHC-I to the TGN is defined by three mutant Nefs (^{62}AAAA^{65}, ^{72}AXXA^{75}, and M20A) that all are crippled for MHC-I downregulation.

The last step of the NPA model partially overlaps with an alternative model in which Nef, the cytoplasmic domain of MHC-I, and AP-1 form a ternary complex (termed the NMA model). This complex is proposed by two groups (24, 35) to block MHC-I migration from the TGN to the cell surface. A telling distinction between the NPA and NMA models is the role of ^{62}EEEE^{65}. In the NPA model, ^{62}EEEE^{65} is the decisive binding element in Nef to engage both PACS-1 and PACS-2. In the NMA model, ^{62}EEEE^{65} has the subsidiary role of stabilizing the Nef, MHC-I cytoplasmic domain, and AP-1 complex in conjunction with P78 and possibly M20. We have undertaken an evaluation of these two models by a detailed mutational analysis of the functional significance of the ^{62}EEEE^{65} domain in Nef.

* Corresponding author. Mailing address: Y9.206, Department of Internal Medicine, UT Southwestern Medical Center, 5323 Harry Hines Boulevard, Dallas, TX 75390. Phone: (214) 648-9970. Fax: (214) 648-0231. E-mail: victor.garcia@utsouthwestern.edu.

▽ Published ahead of print on 23 July 2008.

MATERIALS AND METHODS

In vitro binding assays. BL-21 pLysS cells were transformed with pGEX2TSF2Nef, pGEX2TfurinCD (furin amino acids 739 to 794), pET32fbr (PACS-1 amino acids 117 to 266), and pET28HckSH3 (Hck amino acids 61 to 117). A 2-ml starter culture was initiated from a single colony and grown at 37°C with shaking to an optical density at 600 nm of 0.8. The starter culture then was used to inoculate 50 ml of Luria-Bertani medium with the appropriate antibiotics and grown until the culture reached an optical density at 600 nm of 0.6. Isopropyl-β-D-thiogalactopyranoside (1 mM) was added to the culture for a 3-h induction of the protein. Cultures were pelleted and stored frozen at −20°C.

Pellets containing the glutathione *S*-transferase (GST) fusion proteins were resuspended in 10 ml of phosphate-buffered saline (PBS) supplemented with a protease inhibitor tablet (Roche). A concentration of 50 μg/ml of lysozyme (Roche) was added to these resuspensions for 15 min at room temperature. The resuspended bacteria then were sonicated (with a Fisher 550 sonic dismembrator) on ice using a microtip for 1 min at power setting 3.5 and a 10-s on, 10-s off pulse program. Bacterial lysates then were cleared by centrifugation at 13,000 × *g* at 4°C for 20 min. Supernatant then was incubated with 0.5 ml of packed glutathione Sepharose beads for 30 min at room temperature on a rotator. This suspension then was loaded into a column. The beads then were washed with 10 ml of cold PBS three times. The bound protein was eluted with 10 mM reduced glutathione followed by exhaustive dialysis. The protein concentration was determined by the Bradford assay (Bio-Rad).

Bacterial pellets containing histidine-tagged proteins were resuspended in 10 ml of 1× nickel-nitrilotriacetic acid (Ni-NTA) bind buffer (Novagen Ni-NTA buffer kit) along with 50 μg/ml lysozyme and a protease inhibitor tablet (Roche) for 15 min at room temperature. The supernatant was incubated with 1 ml of Ni-NTA beads for 1 h at 4°C. The beads were loaded onto a column and washed with 1× Ni-NTA bind buffer plus 20 mM imidazole three times. Protein was eluted with 1× Ni-NTA bind buffer containing 250 mM imidazole, the purity was assessed by sodium dodecyl sulfate-polyacrylamide gel electrophoresis (SDS-PAGE), and the protein concentration was determined.

Purified proteins were combined at 3 μM each in 0.5 ml of binding buffer (50 mM Tris, pH 7.5, 1% IGEPAL CA-630, 2 mM $MgCl_2$, and 200 mM NaCl). Binding reactions were done at room temperature or 4°C for 1 h, followed by 30 min of rotation with 50 μl glutathione Sepharose beads. Protein isolated on the beads was washed twice with binding buffer, once with 1 M NaCl, and twice more with binding buffer. All washes were done at 4°C. Protein was eluted with SDS sample buffer, resolved by SDS-PAGE, and analyzed by Western blotting with polyclonal anti-polyhistidine (Abcam).

Cell lines and culture conditions. Suspension cells were maintained in complete RPMI in a 5% CO_2 incubator, and adherent cells were maintained in complete Dulbecco's modified Eagle's medium in a 10% CO_2 incubator. Complete medium included 10% fetal bovine serum (FBS), 50 IU/ml of penicillin, 50 μg/ml streptomycin, 2 mM glutamine; for suspension cells, it also was supplemented with 1 mM sodium pyruvate.

Expression vectors. Mutated SF2Nef coding sequences were made by site-directed mutagenesis (Stratagene). The SF2Nefs with two alanines introduced into the Nef AC were provided by C. Cheng-Mayer (34). These coding sequences were introduced into pLXSN, pcDNA3.1, and the SF2 proviral molecular clone, p9B18, by standard cloning methods.

Transductions. 293T cells were transfected with 2 μg of the amphotropic packaging vector pEQPAM and 2 μg of the pLXSN (vector control) or appropriate pLNefSN vector with Lipofectamine 2000 (Invitrogen). Medium was harvested approximately 48 h posttransfection by being filtered through a 0.45-μm filter (Nalgene). A 24-well plate was coated with 40 μg/well retronectin (Takara Biomedicals, Kyoto, Japan). After 2 h at room temperature, the retronectin was removed, 0.5 ml 2% bovine serum albumin in PBS was added for 30 min at room temperature, and the wells were washed once with PBS (0.5 ml). Filtrate containing amphotrophic vector then was added and left on the plate for 45 min at 37°C, and then this procedure was repeated. CEM cells (300,000) were transduced by the retronectin-bound retroviral vector in 0.5 ml of complete RPMI overnight at 37°C. An additional 0.5 ml of vector was added the next day. On the following day, the cells were resuspended in a 12-well plate containing 1.5 mg/ml G418 (Gibco) in a final volume of 2 ml. After 48 h, the cells were replated in a 6-well plate and 1 ml of medium with G418 was added. Transduced cells then were expanded into a T75 flask without G418 for subsequent analysis.

Cell staining and flow cytometry. Cells (500,000) were labeled with anti-HLA-A1,11,26 (One Lambda, Inc.) at 4°C. HLA-A1 is endogenously expressed by CEM T cells. Cells then were washed twice with 2 ml fluorescence-activated cell sorter buffer (PBS supplemented with 4% FBS), and 2 μl of fluorescein isothiocyanate-conjugated goat anti-mouse immunoglobulin M (Biosource) was added for 20 min at 4°C. Washings were repeated, and then 10 μg of mouse immunoglobulin G antibody (Sigma) was used as the block (20 min at 4°C). Washings were repeated, and 7 μl of mouse anti-CD4-phycoerythrin (Exα) was added (20 min at 4°C). Washings were repeated, and the cells were resuspended in 200 μl fluorescence-activated cell sorter buffer plus 200 μl of 2% paraformaldehyde. Cells then were analyzed by a Becton Dickinson FACSCalibur with Cell Quest software. Nef expression levels were monitored by Western blot analysis with sheep anti-SF2Nef antiserum.

PAK2 in vitro kinase assays. PAK2 activation assays were performed with transduced CEM cells (10^6) or 293T cells (1 well of a 6-well plate) transfected with Lipofectamine 2000 to express Nef from pcDNA3.1. The results were the same and were combined for statistical analysis. Cells were washed with PBS and lysed in 50 mM Tris-HCl (pH 8.0), 0.5% IGEPAL CA-630, 10% glycerol, 100 mM NaCl, 2 mM EDTA, 2 mM $NaVO_4$, 2 mM NaF, 20 mM β-glycerophosphate, 25 mM benzamidine, and one Roche protease inhibitor tablet per 10 ml. The supernatant fraction (13,000 × *g*, 10 min) of whole-cell lysates (600 μg protein) was incubated in lysis buffer with 10 μl of sheep anti-HIV Nef antibody in a final volume of 800 μl for 1.5 h on ice. Protein A beads (40 μl) then were added to the lysate and rotated for 2 h at 4°C. Beads were centrifuged, washed twice with cold lysis buffer, washed once with 1 M $MgCl_2$, and washed twice with kinase buffer containing 50 mM Tris-HCl (pH 7.5), 5 mM $MgCl_2$, 100 mM NaCl, 1% Triton X-100. Beads were resuspended in 100 μl of room temperature kinase buffer. [γ-^{32}P]ATP (30 μCi at 3,000 Ci/mmol) was added to the beads for 10 min at 30°C. Reactions were stopped with 10 μl of 0.5 M EDTA, the beads were centrifuged, and supernatant was removed. One hundred microliters of 1.5× SDS loading buffer was added to the beads, and eluted protein was heated at 95°C for 5 min. Proteins were electrophoretically separated on SDS–10% PAGE gels. Dried gels were analyzed using a Cyclone storage phosphor system (Packard) with the Optiquant image analysis program.

Production of HIV-1. Two micrograms of the SF2 proviral molecular clone p9B18 was transfected with Lipofectamine 2000 into 293T cells. Virus was harvested 36 to 48 h posttransfection and filtered (filter pore size, 0.45 μm). Levels were quantitated by a $p24^{gag}$ antigen enzyme-linked immunosorbent assay (enzyme immunoassay kit; Beckman Coulter).

HeLa-MAGI infectivity assays. A total of 80,000 HeLa-MAGI cells (17) were seeded in 12-well plates and infected 24 h later in triplicate with 5 ng of $p24^{gag}$ in 400 μl of cell culture medium containing 20 μg/ml of DEAE-dextran (Sigma). At 2 h postinoculation, 1 ml of culture medium was added, and the cells were incubated for an additional 36 h. The cells then were fixed with 1% formaldehyde and 0.2% glutaraldehyde in PBS for 5 min at room temperature and stained with a solution composed of 4 mM potassium ferrocyanide, 4 mM potassium ferricyanide, 2 mM $MgCl_2$, and 0.4 mg/ml 5-bromo-4-chloro-3-indolyl β-D-galactopyranoside (X-Gal) in PBS. Single and adjacent blue cells were counted as one infection event on an Olympus IX70 microscope.

Statistical analyses. GraphPad Prism (San Diego, CA) version 4.0 was used for the comparison of parameters between groups by the Student's *t* test. Numerical values are expressed as the means ± standard errors of the means.

RESULTS

The direct interaction of PACS-1 and the AC of Nef has been reported to be required for the downregulation of MHC-I (5, 27). Therefore, a fine-structure mutational analysis of the Nef AC should result in a strong correlation between in vitro binding and MHC-I downregulation activity. Accordingly, we investigated the direct interaction of the fully functional Nef from the proviral clone SF2 (SF2Nef) with the fbr of PACS-1 (5). GST-SF2Nef fusion protein was incubated at 4°C with a histidine-tagged fragment of PACS-1 containing the 17-kDa furin binding domain (ht-fbr) with both proteins at 3 μM. We found much less than 1% of the input ht-fbr bound to GST-SF2Nef (Fig. 1A). In light of the weak binding of Nef to the fbr, we included positive controls for the functionality of the ht-fbr and GST-SF2Nef proteins. We first assayed the binding of the furin cytoplasmic tail to ht-fbr (Fig. 1A). As previously reported, the phosphorylation mimic form of the furin AC (^{773}DDDEEDE^{779}, GST-furin tail DDD) binds strongly to the ht-fbr, but the dephosphorylated form (^{773}SDSEEDE^{779}, GST-

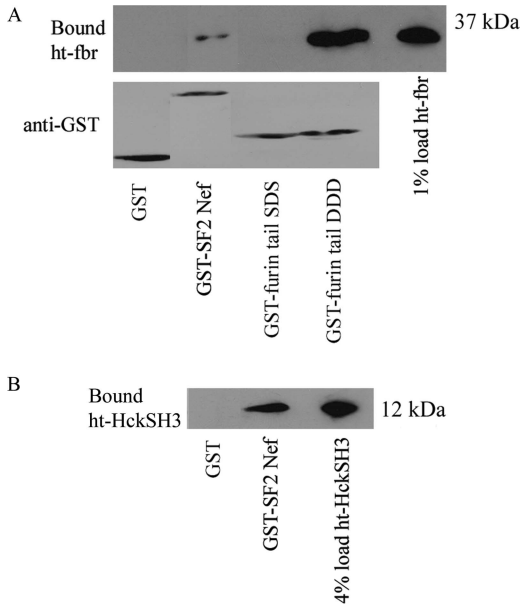

FIG. 1. In vitro binding between ht-fbr and GST-SF2Nef. (A) In vitro binding reactions utilizing purified proteins from bacteria were performed with PACS-1 ht-fbr and a GST fusion protein. A Western blot to detect bound ht-fbr is shown at the top. Lane 1, GST negative control; lane 2, GST-SF2Nef fusion protein; lane 3, GST-furin tail SDS (dephosphorylated AC); lane 4, GST-furin tail DDD (phosphorylation mimic AC); and lane 5, loading control of 1% of the ht-fbr input. The lower panel is a Western blot with anti-GST. (B) In vitro binding reaction with GST-SF2Nef fusion protein and histidine-tagged Hck SH3 domain (ht-HckSH3). Lane 1, GST negative control; lane 2, GST-SF2Nef fusion protein; and lane 3, loading control of 4% of the ht-HckSH3 input.

furin tail SDS) does not (33). The level of specific binding of the phosphorylation mimic form to ht-fbr was much higher than that observed for SF2Nef. To address the possibility that our GST-SF2Nef protein was defective, GST-SF2Nef was bound to the histidine-tagged SH3 domain of Hck (18). The interaction between SF2Nef and ht-HckSH3 resulted in a strong association (Fig. 1B). Although we did not observe sufficiently strong binding in vitro to suggest that the Nef-PACS-1 interaction has functional significance (26), the possibility remains that Nef indirectly binds PACS-1 intracellularly.

In the absence of a strong Nef-fbr interaction in vitro, we turned to a detailed analysis of the functional impact of mutating the Nef AC. Our starting point was the quadruple mutant with all four glutamates converted to alanine (^{62}AAAA^{65}) that is known to lack the ability to downregulate MHC-I (10). Less drastic mutations have not been investigated, nor has the impact of the ^{62}AAAA^{65} mutation been extensively characterized with regard to other Nef functions. Therefore, we analyzed SF2Nefs with two glutamates mutated to alanine (SF2NefAAEE, SF2NefEAAE, and SF2NefEEAA) with the expectation that two acidic residues would not constitute an AC. These double mutants along with SF2NefAAAA were expressed in the CEM T-cell line by retroviral transduction and were analyzed by flow cytometry. That the quadruple mutant SF2NefAAAA fails to downregulate the cell surface MHC-I was confirmed, but to our surprise the three doubly mutated Nefs were fully functional for MHC-I downregulation (Fig. 2A, C). These four mutant Nefs downregulated CD4 and exhibited levels of protein expression equivalent to that of SF2Nef (Fig. 2A, B, and D). To complete this mutational approach, we made the four triply mutated Nefs retaining only a single glutamate (SF2NefAAAE, SF2NefAAEA, SF2NefAEAA, and SF2NefEAAA). These Nefs exhibited between 39.3% ± 6.4% and 55.3% ± 4.9% of wild-type activity in downregulating MHC-I relative to the levels for the parental SF2Nef. However, their CD4 downregulation activity and levels of expression were not affected.

Together, these findings indicated that ^{62}EEEE^{65} is unlikely to represent a region of Nef that interacts with high specificity to PACS-1. Of particular import is the fact that only two glutamates are required for full function, and as shown by SF2NefEAAE, the glutamates do not have to be contiguous. Also, it is unlikely that any of the individual E residues is specifically interacting with the PACS-1 AC binding site, since the four possible SF2Nefs with a single E in this region all exhibit similar partial function. Nonetheless, an interesting feature of the putative Nef AC is the predominance of glutamate over aspartate. In an extensive database of 1,643 subtype B Nefs, approximately 90% of the residues in the AC are E, with only 5% being D (25). Therefore, we hypothesized that if Nef AC-mediated MHC-I downregulation is a crucial function, then replacing the four glutamates with aspartates (^{62}DDDD^{65}) should result in less than full activity. Instead, we found SF2NefDDDD to be fully functional for both MHC-I and CD4 downregulation (Fig. 2). Thus, the results shown in Fig. 2 imply that two negative charges that can vary in position are all that is required in this region for Nef to downregulate MHC-I.

Based on the results described above, we postulated that the Nef AC has a more generalized role involving multiple Nef functions. This was tested by characterizing the impact of the above-described mutant Nefs on p21-activated protein kinase 2 (PAK2) activation and the enhancement of infectivity. At 30% ± 8% of wild-type activity, the ^{62}AAAA^{65} mutant was significantly defective for PAK2 activation (Fig. 3A, B). While Nefs with two E residues were capable of fully (or nearly so) activating PAK2, the mutants with a single E gave a more complex pattern. SF2NefAAAA exhibited about a quarter of the wild-type enhancement of infectivity. Single-E Nefs exhibited between 43% ± 14% and 58% ± 10% of the wild-type enhancement of infectivity (Fig. 3C). We also observed that the activation of PAK2 shows a preference for glutamates over aspartates, since the SF2NefDDDD mutant at 38% ± 7% activity of the wild type is significantly defective (Fig. 3B). SF2NefDDDD also is partially defective for the enhancement of infectivity (68% ± 4% [n = 3] of the level for wild-type SF2Nef; data not shown). The latter observations may account for the fact that glutamates are preferred in this region of the protein over aspartates.

The concept of the AC strongly implies that substituting basic residues for acidic residues would greatly impair function. This consideration was incorporated into the original definition of the AC, and no known ACs include K or R (23, 32). To test this prediction, we constructed four mutant SF2Nefs in which a single K was substituted for each of the Es. No significant diminution was observed for MHC-I downregulation except for SF2NefEEEK, which was half as active as

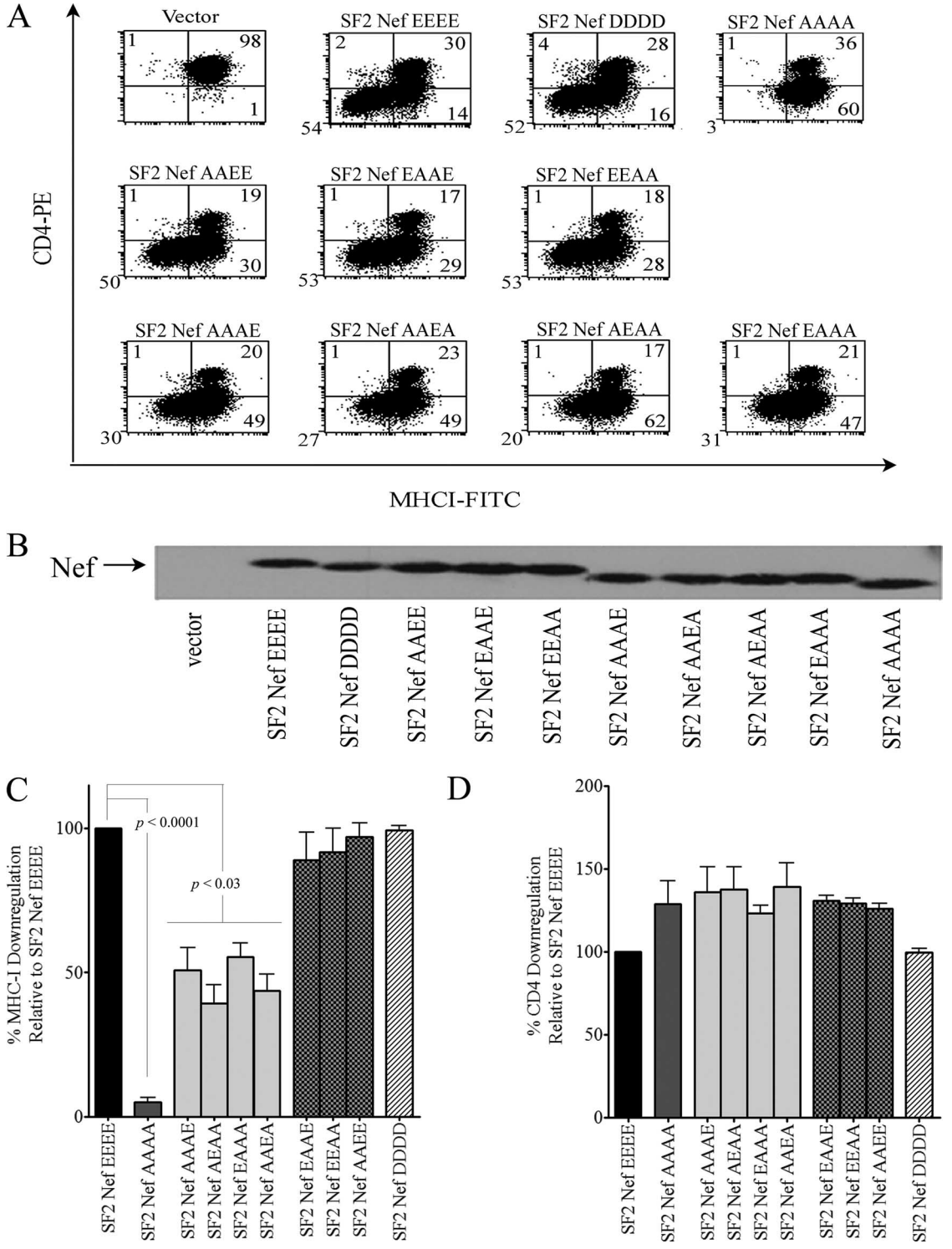

FIG. 2. Effects of reducing the negative charge within the Nef AC on Nef-mediated MHC-I and CD4 downregulation. Nine SF2Nef AC mutants in addition to the wild-type SF2Nef were stably expressed in CEM cells, and the activity of these Nefs in MHC-I and CD4 downregulation was determined. (A) Two-color analysis for CD4 and MHC-I cell surface expression by flow cytometry. The negative vector control (LXSN) is shown in the upper left. (B) Western blot analysis of Nef expression in extracts from transduced CEM cells. (C) The MHC-I downregulation phenotypes of the Nef AC mutants and the wild-type SF2Nef were analyzed; results are means ± standard errors of the means from at least three independent experiments. The percentage of cells downregulating MHC-I by SF2Nef was set at 100. (D) The CD4 downregulation phenotypes were analyzed as described for panel C. FITC, fluorescein isothiocyanate; PE, phycoerythrin.

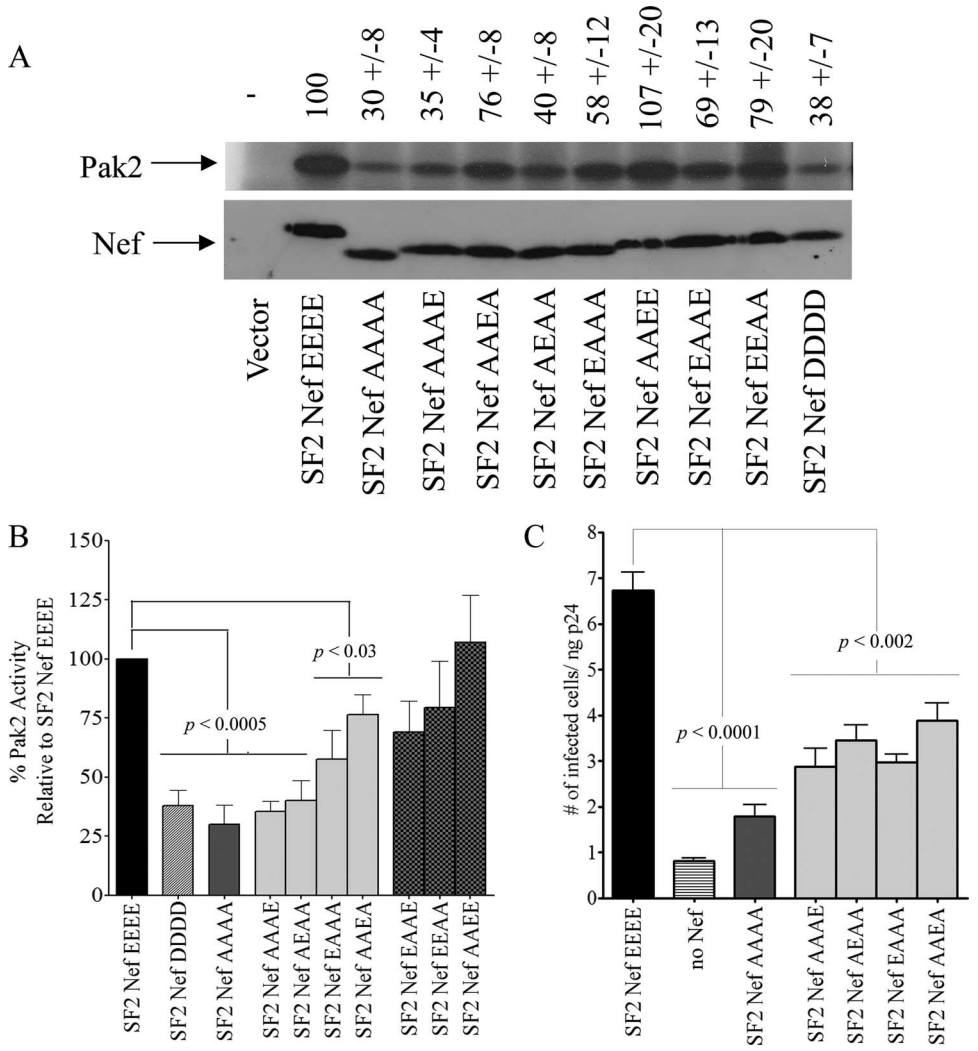

FIG. 3. Effects of reducing the negative charge within the Nef AC on Nef-mediated PAK2 activation and infectivity enhancement. (A) Nine SF2Nef AC mutants in addition to the wild-type SF2Nef were stably expressed in CEM cells or transiently expressed in 293T cells. The activation of PAK2 by Nef was assayed from extracts of these cells by an in vitro kinase reaction (top). The activity of SF2Nef was set to 100. The negative control (Vector) represents CEM cells transduced with LXSN or 293T cells transfected with pcDNA3.1. The bottom panel is a Western blot analysis of Nef expression in these extracts. (B) A Student's *t* test was used to compare the PAK2 activation by nine AC mutant Nef proteins. The activation of PAK2 by SF2Nef was set to 100. Note that mutated Nefs are grouped by statistical significance. (C) The SF2 molecular clones, p9B18, p9B18Nef(−), and p9B18 with mutated Nefs were analyzed for their ability to enhance infectivity in a single-round infectivity assay of target HeLa-MAGI cells ($n = 6$).

SF2Nef for MHC-I downregulation (Fig. 4A). A small reduction (59% ± 22% of wild-type activity) in the ability of Nef to activate PAK2 also was observed for SF2NefEEEK (Fig. 4B, C). In all cases, the single-K mutations had no effect on CD4 downregulation (Fig. 4C). Again, these results do not support the concept that the four contiguous Es function as an AC in the sense that the bona fide AC in furin serves as a trafficking signal by binding PACS-1. However, Agopian et al. (1) have reported a primary brain isolate, 14ANef, with an AC of ^{62}KEEE^{65} that is defective in MHC-I downregulation. Our results shown in Fig. 4A suggest that K62 does not account for the MHC-I downregulation defect in 14ANef. We confirmed that 14ANef is nonfunctional for MHC-I downregulation, but that the mutation of K62 to E (14ANefK62E) had only 12% ± 4% ($n = 3$) of the MHC-I downregulation activity of SF2Nef (not shown). Therefore, we attribute the defect in 14ANef to an amino acid(s) outside of the putative Nef AC.

Although it appears unlikely that the four-glutamate Nef AC (6, 13) functions as a decisive structural element for Nef to bind PACS-1 in the manner of the furin AC, we considered the possibility that the structure of the Nef AC corresponds to that of ACs containing five negative residues within a stretch of 10 amino acids with no requirement for phosphoserine or phosphothreonine (23, 32). Thus, we postulated a mechanism of Nef AC function distinct from that of the furin AC. For Nef, this would require adding E59, which is 95% conserved (25). This inclusion would yield a Nef AC extending from amino acid residues 59 to 65 (EAQEEEE). To test this alternate hypothesis, we made SF2NefE59A and the triple mutants SF2NefE59A/AAEE, SF2NefE59A/EAAE, and SF2NefE59A/

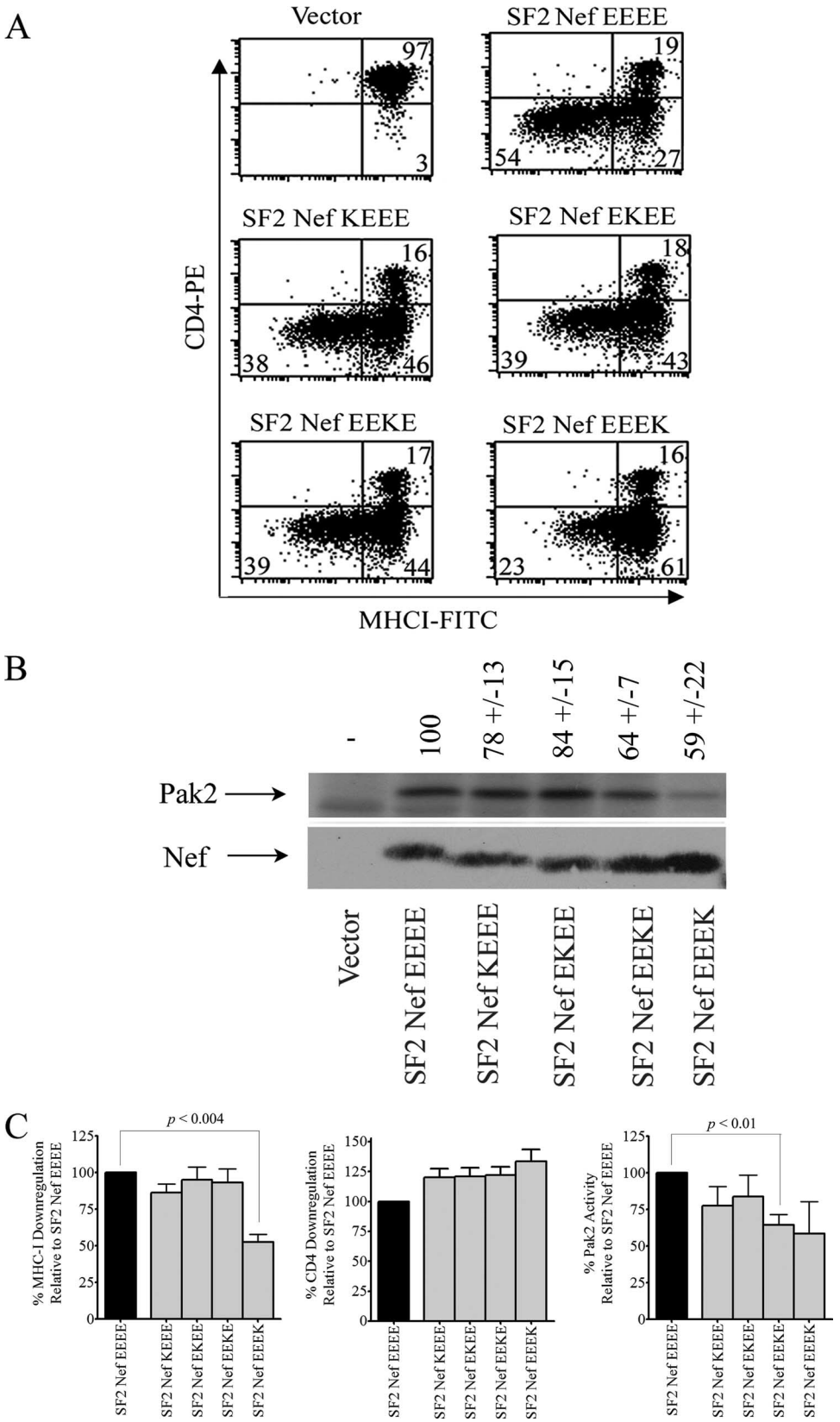

FIG. 4. Effects of a positively charged residue in the Nef AC on the downregulation of MHC-I. (A) CEM T cells transduced with vector alone (LXSN), wild-type SF2Nef, or SF2Nef with a lysine substitution for each of the individual core components of the Nef AC (^{62}KEEE^{65}, ^{62}EKEE^{65}, ^{62}EEKE^{65}, and ^{62}EEEK^{65}). Cells were stained for surface MHC-I and CD4 and were analyzed by flow cytometry. A representative example is shown from one of four independent experiments. (B) The top panel represents the effect of a basic residue in the Nef AC on the activation of

EEAA. As demonstrated in Fig. 5, the single mutation E59A had no effect on the downregulation of MHC-I or CD4. In the case of the double mutants plus E59A, there were only small negative effects on the downregulation of MHC-I compared to those of the corresponding double mutants (Fig. 5C), which leads us to conclude that E59 is not a significant part of a functional AC.

We next tried to discern a mechanistic link between bona fide ACs that serve as trafficking signals and the ability of Nef to downregulate MHC-I by inserting the canonical furin AC into Nef. Three *nef* constructs were made in which amino acids 59 to 65 (EAQEEEE) were replaced with the furin AC wild-type sequence (SDSEEDE), the phosphorylation mimic form (DDDEEDE), and the constitutively dephosphorylated form (ADAEEDE). If a bona fide AC is able to function in the context of the Nef protein, then one would expect that a Nef containing the dephosphorylated form of the furin AC would fail to interact with PACS-1 (Fig. 1A) and, as a result, would be inactive for MHC-I downregulation. Instead, we observed that all three Nefs containing the furin-like ACs were fully functional for MHC-I downregulation (Fig. 6). Therefore, the furin AC sequence is not functioning in the Nef context as it does in furin, and we conclude that SF2NefADAEEDE is capable of downregulating MHC-I because it contains at least two negative charges within amino acid positions 62 to 65. To be sure that the functional sequence in these three constructs was the last four amino acids (EEDE), we tested SF2NefE64D (i.e., ^{59}EAQEEDE^{65}), which was, as expected, fully active for MHC-I and CD4 downregulation (data not shown).

An unexpected result was that the above-described Nefs mutated in A60 (to D) and Q61 (to S, D, or A) were entirely incompetent for CD4 downregulation (Fig. 6). SF2NefA60D and SF2NefQ61A were constructed and tested for their ability to downregulate CD4. SF2NefA60D failed to downregulate CD4, but SF2NefQ61A was fully active. Both of these point mutations were wild type for MHC-I downregulation, demonstrating that the segment immediately N terminal to ^{62}EEEE^{65} is not involved in MHC-I downregulation (data not shown).

In the NMA model, ^{62}EEEE^{65} has the relatively modest role of stabilizing the Nef/MHC-I cytoplasmic domain/AP-1 ternary complex by interacting with the positively charged surface of AP-1 (24, 35). This proposed stabilizing role would allow for considerable flexibility in AC structure. We tested this possibility with charge-neutral alterations in the Nef AC secondary structure. We have previously shown that extending the Nef AC to five residues yields a fully functional Nef (25); therefore, prolines were inserted before, in the middle of, and after ^{62}EEEE^{65}, and these Nefs (PEEEE, EEPEE, and EEEEP) were analyzed for MHC-I and CD4 downregulation. All three of these constructs were expressed at levels comparable to those of the wild type and displayed at least 70% of wild-type activity for MHC-I downregulation, but in contrast to all other AC mutants, they were partially defective for the CD4 downregulation phenotype (data not shown).

In summary, we have found complex structure-function relations for the Nef AC that are most pointedly demonstrated by the facts that SF2NefAAAA is defective for MHC-I downregulation, PAK2 activation, and the enhancement of infectivity but fully functional for CD4 downregulation; SF2NefDDDD is defective for PAK2 activation, partially defective for the enhancement of infectivity, but fully functional for MHC-I and CD4 downregulation; and SF2Nefs with their ACs conformationally disrupted by proline are partially defective for CD4 downregulation but are wild type in their ability to downregulate MHC-I.

DISCUSSION

A PACS-1 binding motif called an AC is present in the cytoplasmic domain of many membrane-spanning proteins (23, 30). The canonical AC in furin (SDSEEDE) is phosphorylated and activated by casein kinase 2 at the two serines to give seven negatively charged residues in a row. Thomas and coworkers (5, 6, 13) have proposed that Nef contains a four-residue AC (^{62}EEEE^{65}) that specifically binds Nef to PACS-1 and PACS-2, and that this binding is crucial for Nef to downregulate MHC-I (the NPA model). We have shown that SF2NefE64D downregulates MHC-I, which is consistent with the Nef AC being functionally the same as the last four amino acids of the furin AC. However, the relevance of the furin AC as a model for the Nef AC has been called into question recently. Interpreting the results of Lubben et al. (20), Atkins and coworkers (5) have suggested that the EEDE sequence of the furin AC is not required for furin to bind to PACS-1. However, the Nef AC has no casein kinase 2 phosphorylation sites; therefore, there is no other basis for its binding to PACS-1 other than ^{62}EEEE^{65}. Indeed, in accord with the above suggestion, we find that the in vitro binding of the short Nef AC to the furin binding domain of PACS-1 is very weak compared to that of the long furin cytoplasmic tail AC (Fig. 1). An alternate possibility is that the Nef AC consists of five glutamates (^{59}EAQEEEE^{65}), but mutational analysis demonstrated that E59 is at best marginally involved in the downregulation of MHC-I (Fig. 5). Further, the incorporation of the bona fide furin AC into Nef resulted in the loss of the regulatory properties of the furin AC (Fig. 6). Mutational studies demonstrated that the Nef downregulation of MHC-I requires only a net of two negative charges in Nef's putative AC (Fig. 2 and 4), and we also noted that the quadruple mutation of ^{62}EEEE^{65} to ^{62}AAAA^{65} exhibits multiple functional defects in addition to that of MHC-I downregulation (Fig. 3). In sum, our efforts to mechanistically define AC function in Nef have been unsuccessful, other than confirming the inability of the quadruple mutation (SF2NefAAAA) to downregulate MHC-I.

The lack of experimental support for the assigned role of

PAK2. PAK2 activity was assayed from extracts of transduced CEM. The PAK2 activity of SF2Nef was set to 100. The negative control represents cells transduced with vector (LXSN). The bottom panel is a Western blot analysis of Nef expression in these extracts. (C) The average of four independent experiments was used to determine the effect of lysine substitutions in the AC on the percentage of cells downregulating either MHC-I (left) or CD4 (middle) or the activation of PAK2 by Nef (right), and the effects of the mutants compared to that of wild-type SF2Nef were analyzed by Student's *t* test. FITC, fluorescein isothiocyanate; PE, phycoerythrin.

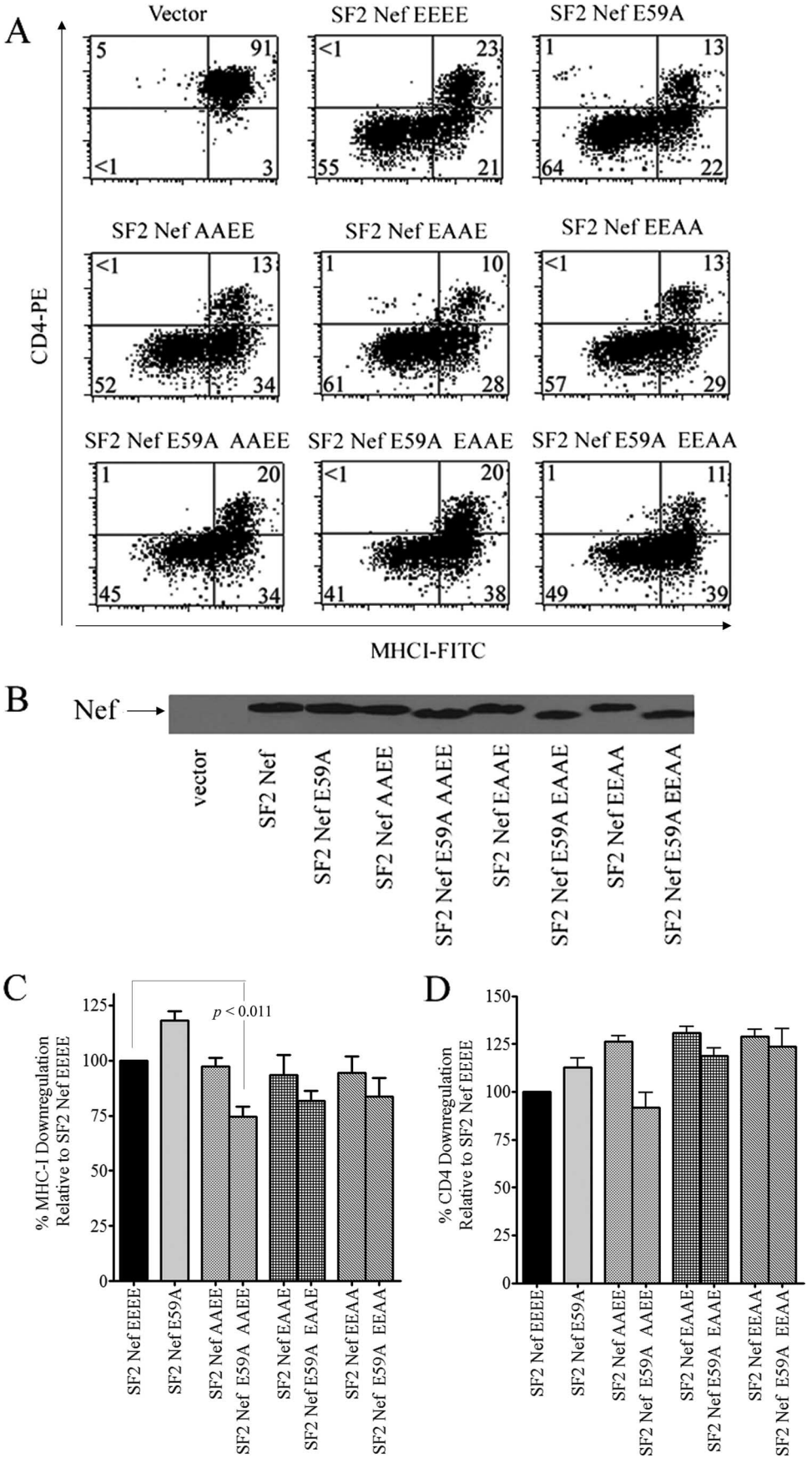
A
Vector
SF2 Nef EEEE
SF2 Nef E59A
SF2 Nef AAEE
SF2 Nef EAAE
SF2 Nef EEAA
SF2 Nef E59A AAEE
SF2 Nef E59A EAAE
SF2 Nef E59A EEAA
CD4-PE
MHCI-FITC
B
Nef
vector
SF2 Nef
SF2 Nef E59A
SF2 Nef AAEE
SF2 Nef E59A AAEE
SF2 Nef EAAE
SF2 Nef E59A EAAE
SF2 Nef EEAA
SF2 Nef E59A EEAA
C
% MHC-I Downregulation Relative to SF2 Nef EEEE
p < 0.011
D
% CD4 Downregulation Relative to SF2 Nef EEEE
SF2 Nef EEEE
SF2 Nef E59A
SF2 Nef AAEE
SF2 Nef E59A AAEE
SF2 Nef EAAE
SF2 Nef E59A EAAE
SF2 Nef EEAA
SF2 Nef E59A EEAA

^{62}EEEE^{65} in the NPA model led us to consider the models of Noviello and coworkers (24) and Wonderlich and coworkers (35). In these highly similar models (the NMA models), the Nef AC is proposed to have a stabilizing effect on the formation of a ternary complex among Nef, MHC-I cytoplasmic domain, and AP-1. As a stabilizing factor, it is distinctly possible that the Nef AC tolerates a high degree of structural flexibility and is still functional. To test for the possible structural flexibility of the Nef AC, we have induced altered conformations in the Nef AC by inserting prolines (PEEEE, EEPEE, and EEEEP) and found little effect on the ability of Nef to downregulate MHC-I, although variable negative effects were found for CD4 downregulation. Therefore, our investigations support the role assigned to the Nef AC by the NMA model.

In addition to different roles for the Nef AC in the NPA and NMA models, the two models also differ with regard to the importance of the enhanced endocytosis of MHC-I. In the NPA model, a complex train of events accelerates the internalization of MHC-I from the plasma membrane. For example, Blagoveshchenskaya et al. (6) report a twofold increase in the MHC-I internalization of externally labeled MHC-I molecules in HeLa-CD4 cells that express Nef relative to that of control cells. This enhanced internalization levels off at a 10% reduction of the cell surface label by 10 min. An alternate interpretation of this quick cessation in the internalization of label is that a rapid equilibration of labeled cell surface protein with a small unlabeled intracellular pool by a recycling process results in a slight dilution of label on the cell surface (22, 28). A small effect on MHC-I recycling is unlikely to play a significant role in Nef-induced MHC-I downregulation (14). In the NMA model, the internalization of cell surface MHC-I does not have a significant role. Instead, Nef diverts newly synthesized MHC-I off the default pathway (to the plasma membrane) to the paranuclear region of the cell (15, 20, 29).

The mechanism of the downregulation of MHC-I in the NMA model is that Nef forms a binding site for AP-1 that minimally contains the MHC-I cytoplasmic tail, ^{62}EEEE^{65}, and P78 (24, 35). AP-1 is then the effecter that reroutes MHC-I from its normal transport to the plasma membrane (29). Both groups observed that the ^{62}AAAA^{65} mutation blocked ternary-complex formation, leading to the suggestion that the tetraglutamate segment of Nef interacts with a cluster of positive charges present on the AP-1 subunit μ1. We find this proposal to be consistent with our results, in that in the NMA model the tetraglutamate segment of Nef plays a contributing role as part of a cooperative interaction with AP-1 instead of being the decisive determinant in the binding of Nef to PACS-1 and PACS-2. Therefore, P78 (and possibly other yet-to-be-identified Nef residues) and the cytoplasmic tail of MHC-I could form a weak binding site for AP-1 that requires stabilization by the negative charges of the tetraglutamate segment, with two glutamates sufficiently stabilizing the interaction to allow for full function

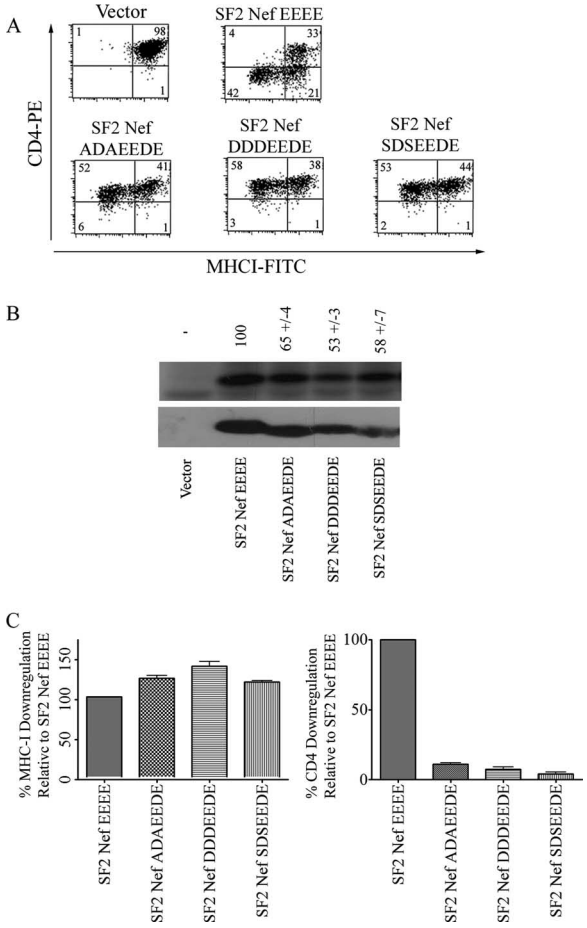

FIG. 6. Analysis of the activity of the furin AC substituted for the AC in Nef. The sequence of a nonphosphorylatable form of the furin AC (ADAEEDE), a phosphorylation mimic form (DDDEEDE), and the native furin AC sequence (SDSEEDE) were substituted for Nef amino acid residues 59 to 65. (A) Flow cytometric analyses of the MHC-I and CD4 surface expression of CEM cells transduced with wild-type SF2Nef and SF2Nefs containing furin AC sequences of Nef are depicted. (B) The furin AC sequences on the Nef background, in addition to the wild-type SF2Nef, were stably expressed in CEM cells, and the activation of PAK2 by Nef was assayed from extracts of these cells by an in vitro kinase reaction in the top panel. The PAK2 activation of SF2Nef was set to 100. The negative control represents cells transduced with vector alone (LXSN). Western blot analysis of Nef proteins present in cell lysates is shown in the lower panel. (C) A graphical analysis of the effects of substituting the furin AC on Nef-mediated MHC-I (left panel) and CD4 (right panel) downregulation. The downregulation of wild-type SF2Nef was set to 100%. FITC, fluorescein isothiocyanate; PE, phycoerythrin.

FIG. 5. Analysis of the role of glutamate 59 in the downregulation of MHC-I by Nef. (A) CEM cells transduced with vector alone, wild-type SF2Nef, SF2Nef E59A, SF2Nef double mutants (^{62}AAEE^{65}, ^{62}EAAE^{65}, and ^{62}EEAA^{65}), or SF2Nef E59A on the background of the double mutants (E59A/^{62}AAEE^{65}, E59A/^{62}EAAE^{65}, and E59A/^{62}EEAA^{65}) were stained for surface MHC-I and CD4 and analyzed by flow cytometry. One of three or more independent experiments is shown. (B) Western blot analysis of the expression of the Nef proteins analyzed in panel A. (C) A graphical analysis of the effects of mutating the SF2Nef acidic residue E59 on the background of the double mutants ^{62}AAEE^{65}, ^{62}EAAE^{65}, and ^{62}EEAA^{65} on Nef-mediated MHC-I (C) and CD4 (D) downregulation. The value for SF2Nef was set to 100. FITC, fluorescein isothiocyanate; PE, phycoerythrin.

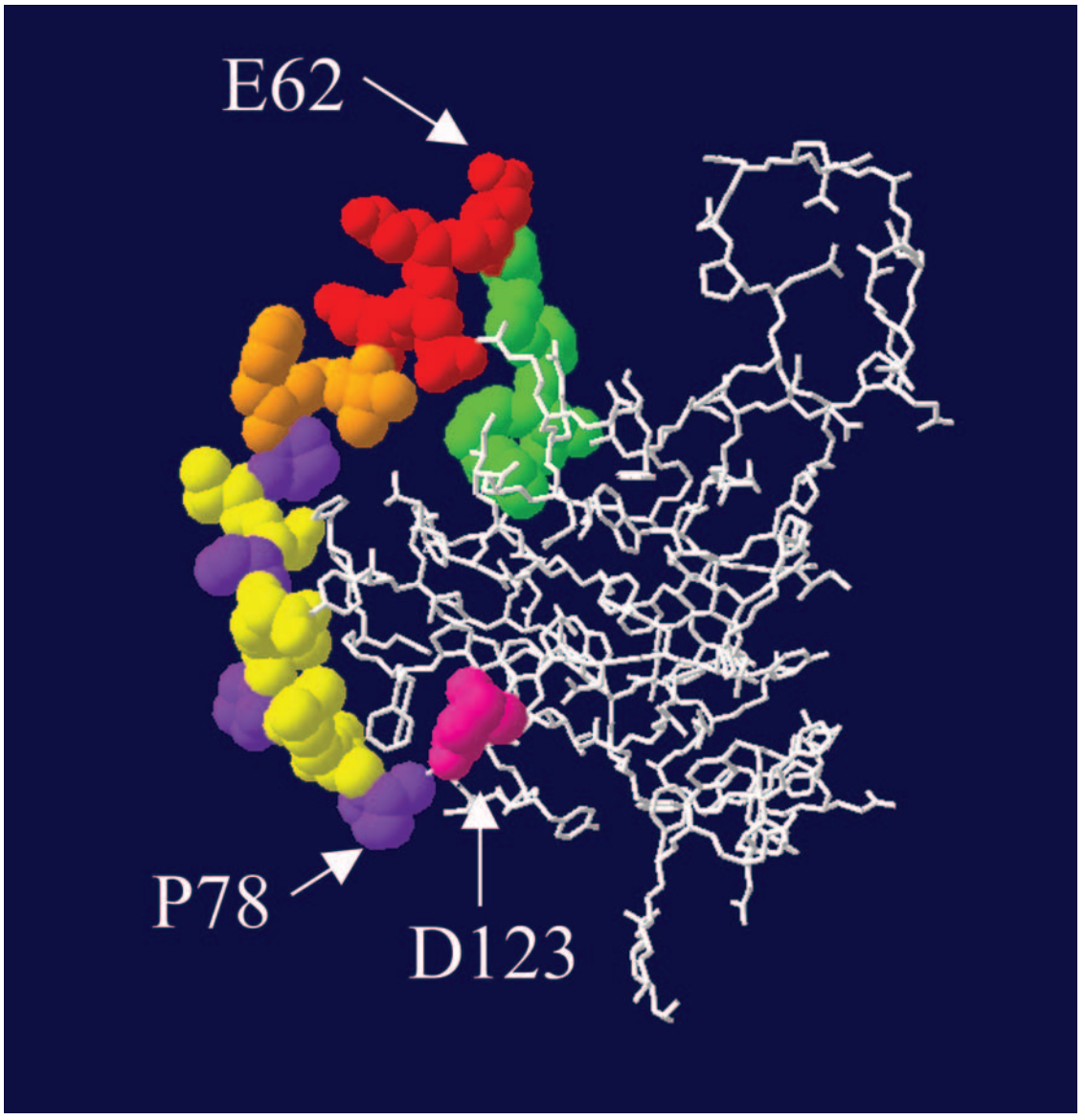

FIG. 7. Location of amino acid residues on the surface of Nef that are necessary for the downregulation of MHC-I. The amino acids mutated in this study are on the surface of the Nef protein (Protein Data Bank entry 2nef). The space-filling, colored residues are the following: green, ^{57}WLEAQ^{61}; red, ^{62}EEEE^{65}; orange, ^{66}VGF^{68}; yellow with prolines in purple, ^{69}PVRPQVPLRP^{78}; and pink, D123.

and a single glutamate resulting in partial function (Fig. 2). In this way, the failure of SF2NefAAAA to downregulate MHC-I can be accounted for independently of an interaction with PACS-1 and elevated rates of MHC-I endocytosis.

In Fig. 7, the amino acids discussed in this paper are displayed on the surface of a three-dimensional presentation of Nef (11). The region that is just N terminal of the Nef AC is looped behind ^{62}EEEE^{65}. Present in the N-terminal segment is amino acid A60, along with W57 and L58. The latter two residues are proposed to directly interact with the cytoplasmic tail of CD4 (12, 21). To the C-terminal side of ^{62}EEEE^{65} are three 99.5% conserved residues, V66, G67, and F68 of unknown function (25), followed by the polyproline tract, ^{69}PVRPQVPLRP^{78}. In general, mutations in the Nef AC and polyproline tract are deleterious for MHC-I downregulation and are partially to wholly defective for PAK2 activation and the enhancement of infectivity but not CD4 downregulation. Amino acids in these regions have been given roles in MHC-I downregulation in both the NPA and NMA models. A crucial Nef residue that has not been included in either the NPA or NMA model is D123. The conservative mutation D123E abrogates MHC-I downregulation, CD4 downregulation, and the enhancement of infectivity but activates PAK2 twofold over wild-type levels (25). It has been suggested previously that the regions on the surface of Nef that are important for MHC-I downregulation and CD4 downregulation are distinct but overlapping and that D123 is in the overlap (7). M20 is not shown in Fig. 7, because it is in the long, flexible N-terminal segment of Nef that is not highly structured. Incorporating all of the structural features of Nef required for MHC-I downregulation will be necessary before a complete mechanism can be described. We are

extending our mutational studies to further characterize the effecter domain on Nef that accounts for MHC-I downregulation.

ACKNOWLEDGMENTS

We are especially grateful to Gary Thomas for his generous contribution of pET32fbr, Kalle Saksela for pGEX-4T-1-Hck-SH3, Cecilia Cheng-Mayer for Nef expression constructs, Paul Luciw for the SF2 proviral clone p9B18, and the NIH AIDS Reference and Research Reagent Program for Nef antibody 2949. We also are greatly appreciative of Alice Shaw for her technical assistance, Daniel Powell for help with flow cytometry, and Paul Denton for his advice on the preparation of figures. Lillian Kuo made Fig. 7.

This work was supported by National Institutes of Health grant AI-33331 (J.V.G.).

REFERENCES

1. **Agopian, K., B. L. Wei, J. V. Garcia, and D. Gabuzda.** 2007. CD4 and MHC-I downregulation are conserved in primary HIV-1 Nef alleles from brain and lymphoid tissues, but Pak2 activation is highly variable. Virology **358:**119–135.
2. **Akari, H., S. Arold, T. Fukumori, T. Okazaki, K. Strebel, and A. Adachi.** 2000. Nef-induced major histocompatibility complex class I down-regulation is functionally dissociated from its virion incorporation, enhancement of viral infectivity, and CD4 down-regulation. J. Virol. **74:**2907–2912.
3. **Arold, S. T., and A. S. Baur.** 2001. Dynamic Nef and Nef dynamics: how structure could explain the complex activities of this small HIV protein. Trends Biochem. Sci. **26:**356–363.
4. **Arora, V. K., B. L. Fredericksen, and J. V. Garcia.** 2002. Nef: agent of cell subversion. Microbes Infect. **4:**189–199.
5. **Atkins, K. M., L. Thomas, R. T. Youker, M. J. Harriff, F. Pissani, H. You, and G. Thomas.** 2008. HIV-1 NEF binds PACS-2 to assemble a multi-kinase cascade that triggers MHC-I downregulation: analysis using siRNA and knockout mice. J. Biol. Chem. **283:**11772–11784.
6. **Blagoveshchenskaya, A. D., L. Thomas, S. F. Feliciangeli, C. H. Hung, and G. Thomas.** 2002. HIV-1 Nef downregulates MHC-I by a PACS-1- and PI3K-regulated ARF6 endocytic pathway. Cell **111:**853–866.
7. **Cohen, G. B., V. S. Rangan, B. K. Chen, S. Smith, and D. Baltimore.** 2000. The human thioesterase II protein binds to a site on HIV-1 Nef critical for CD4 down-regulation. J. Biol. Chem. **275:**23097–23105.
8. **Foster, J. L., and J. V. Garcia.** 2007. Role of Nef in HIV-1 replication and pathogenesis. Adv. Pharmacol. **55:**389–409.
9. **Gorry, P. R., D. A. McPhee, E. Verity, W. B. Dyer, S. L. Wesselingh, J. Learmont, J. S. Sullivan, M. Roche, J. J. Zaunders, D. Gabuzda, S. M. Crowe, J. Mills, S. R. Lewin, B. J. Brew, A. L. Cunningham, and M. J. Churchill.** 2007. Pathogenicity and immunogenicity of attenuated, nef-deleted HIV-1 strains in vivo. Retrovirology **4:**66.
10. **Greenberg, M. E., A. J. Iafrate, and J. Skowronski.** 1998. The SH3 domain-binding surface and an acidic motif in HIV-1 Nef regulate trafficking of class I MHC complexes. EMBO J. **17:**2777–2789.
11. **Grzesiek, S., A. Bax, J. S. Hu, J. Kaufman, I. Palmer, S. J. Stahl, N. Tjandra, and P. T. Wingfield.** 1997. Refined solution structure and backbone dynamics of HIV-1 Nef. Protein Sci. **6:**1248–1263.
12. **Grzesiek, S., S. J. Stahl, P. T. Wingfield, and A. Bax.** 1996. The CD4 determinant for downregulation by HIV-1 Nef directly binds to Nef. Mapping of the Nef binding surface by NMR. Biochemistry **35:**10256–10261.
13. **Hung, C. H., L. Thomas, C. E. Ruby, K. M. Atkins, N. P. Morris, Z. A. Knight, I. Scholz, E. Barklis, A. D. Weinberg, K. M. Shokat, and G. Thomas.** 2007. HIV-1 Nef assembles a Src family kinase-ZAP-70/Syk-PI3K cascade to downregulate cell-surface MHC-I. Cell Host Microbe **1:**121–133.
14. **Kasper, M. R., and K. L. Collins.** 2003. Nef-mediated disruption of HLA-A2 transport to the cell surface in T cells. J. Virol. **77:**3041–3049.
15. **Kasper, M. R., J. F. Roeth, M. Williams, T. M. Filzen, R. I. Fleis, and K. L. Collins.** 2005. HIV-1 Nef disrupts antigen presentation early in the secretory pathway. J. Biol. Chem. **280:**12840–12848.
16. **Kestler, H. W., III, D. J. Ringler, K. Mori, D. L. Panicali, P. K. Sehgal, M. D. Daniel, and R. C. Desrosiers.** 1991. Importance of the nef gene for maintenance of high virus loads and for development of AIDS. Cell **65:**651–662.
17. **Kimpton, J., and M. Emerman.** 1992. Detection of replication-competent and pseudotyped human immunodeficiency virus with a sensitive cell line on the basis of activation of an integrated beta-galactosidase gene. J. Virol. **66:**2232–2239.
18. **Lee, C. H., B. Leung, M. A. Lemmon, J. Zheng, D. Cowburn, J. Kuriyan, and K. Saksela.** 1995. A single amino acid in the SH3 domain of Hck determines its high affinity and specificity in binding to HIV-1 Nef protein. EMBO J. **14:**5006–5015.
19. **Lindwasser, O. W., R. Chaudhuri, and J. S. Bonifacino.** 2007. Mechanisms of CD4 downregulation by the Nef and Vpu proteins of primate immunodeficiency viruses. Curr. Mol. Med. **7:**171–184.
20. **Lubben, N. B., D. A. Sahlender, A. M. Motley, P. J. Lehner, P. Benaroch, and M. S. Robinson.** 2007. HIV-1 Nef-induced down-regulation of MHC class I requires AP-1 and clathrin but not PACS-1 and is impeded by AP-2. Mol. Biol. Cell **18:**3351–3365.
21. **Mangasarian, A., V. Piguet, J. K. Wang, Y. L. Chen, and D. Trono.** 1999. Nef-induced CD4 and major histocompatibility complex class I (MHC-I) down-regulation are governed by distinct determinants: N-terminal alpha helix and proline repeat of Nef selectively regulate MHC-I trafficking. J. Virol. **73:**1964–1973.
22. **Marsh, M., and A. Pelchen-Matthews.** 1996. Endocytic and exocytic regulation of CD4 expression and function. Curr. Top. Microbiol. Immunol. **205:**107–135.
23. **Molloy, S. S., E. D. Anderson, F. Jean, and G. Thomas.** 1999. Bi-cycling the furin pathway: from TGN localization to pathogen activation and embryogenesis. Trends Cell Biol. **9:**28–35.
24. **Noviello, C. M., S. Benichou, and J. C. Guatelli.** 2008. Cooperative binding of the major histocompatibility complex cytoplasmic domain and human immunodeficiency virus type 1 Nef to the endosomal AP-1 complex via its μ subunit. J. Virol. **82:**1249–1258.
25. **O'Neill, E., L. S. Kuo, J. F. Krisko, D. R. Tomchick, J. V. Garcia, and J. L. Foster.** 2006. Dynamic evolution of the human immunodeficiency virus type 1 pathogenic factor, Nef. J. Virol. **80:**1311–1320.
26. **Phizicky, E. M., and S. Fields.** 1995. Protein-protein interactions: methods for detection and analysis. Microbiol. Rev. **59:**94–123.
27. **Piguet, V., L. Wan, C. Borel, A. Mangasarian, N. Demaurex, G. Thomas, and D. Trono.** 2000. HIV-1 Nef protein binds to the cellular protein PACS-1 to downregulate class I major histocompatibility complexes. Nat. Cell Biol. **2:**163–167.
28. **Reid, P. A., and C. Watts.** 1990. Cycling of cell-surface MHC glycoproteins through primaquine-sensitive intracellular compartments. Nature **346:**655–657.
29. **Roeth, J. F., and K. L. Collins.** 2006. Human immunodeficiency virus type 1 Nef: adapting to intracellular trafficking pathways. Microbiol. Mol. Biol. Rev. **70:**548–563.
30. **Schapiro, F. B., T. T. Soe, W. G. Mallet, and F. R. Maxfield.** 2004. Role of cytoplasmic domain serines in intracellular trafficking of furin. Mol. Biol. Cell **15:**2884–2894.
31. **Schwartz, O., V. Marechal, S. Le Gall, F. Lemonnier, and J. M. Heard.** 1996. Endocytosis of major histocompatibility complex class I molecules is induced by the HIV-1 Nef protein. Nat. Med. **2:**338–342.
32. **Voorhees, P., E. Deignan, E. van Donselaar, J. Humphrey, M. S. Marks, P. J. Peters, and J. S. Bonifacino.** 1995. An acidic sequence within the cytoplasmic domain of furin functions as a determinant of trans-Golgi network localization and internalization from the cell surface. EMBO J. **14:**4961–4975.
33. **Wan, L., S. S. Molloy, L. Thomas, G. Liu, Y. Xiang, S. L. Rybak, and G. Thomas.** 1998. PACS-1 defines a novel gene family of cytosolic sorting proteins required for trans-Golgi network localization. Cell **94:**205–216.
34. **Wiskerchen, M., and C. Cheng-Mayer.** 1996. HIV-1 Nef association with cellular serine kinase correlates with enhanced virion infectivity and efficient proviral DNA synthesis. Virology **224:**292–301.
35. **Wonderlich, E. R., M. Williams, and K. L. Collins.** 2008. The tyrosine binding pocket in the adaptor protein 1 (AP-1) mu1 subunit is necessary for Nef to recruit AP-1 to the major histocompatibility complex class I cytoplasmic tail. J. Biol. Chem. **283:**3011–3022.